

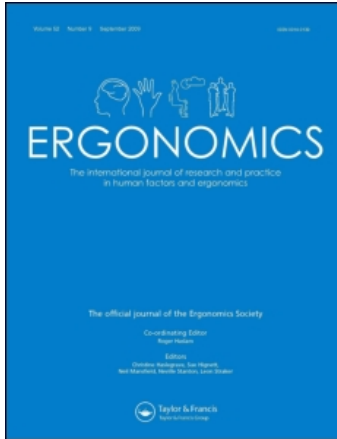
This article was downloaded by: [*Centers for Disease Control and Prevention*]

On: 21 April 2011

Access details: *Access Details: [subscription number 934271632]*

Publisher *Taylor & Francis*

Informa Ltd Registered in England and Wales Registered Number: 1072954 Registered office: Mortimer House, 37-41 Mortimer Street, London W1T 3JH, UK



## **Ergonomics**

Publication details, including instructions for authors and subscription information:

<http://www.informaworld.com/smpp/title~content=t713701117>

### **Estimation of the kinetic energy dissipation in fall-arrest system and manikin during fall impact**

John Z. Wu<sup>a</sup>; John R. Powers<sup>a</sup>; James R. Harris<sup>a</sup>; Christopher S. Pan<sup>a</sup>

<sup>a</sup> National Institute for Occupational Safety and Health, Morgantown, WV, USA

Online publication date: 11 April 2011

**To cite this Article** Wu, John Z. , Powers, John R. , Harris, James R. and Pan, Christopher S.(2011) 'Estimation of the kinetic energy dissipation in fall-arrest system and manikin during fall impact', *Ergonomics*, 54: 4, 367 – 379

**To link to this Article:** DOI: 10.1080/00140139.2010.549966

**URL:** <http://dx.doi.org/10.1080/00140139.2010.549966>

**PLEASE SCROLL DOWN FOR ARTICLE**

Full terms and conditions of use: <http://www.informaworld.com/terms-and-conditions-of-access.pdf>

This article may be used for research, teaching and private study purposes. Any substantial or systematic reproduction, re-distribution, re-selling, loan or sub-licensing, systematic supply or distribution in any form to anyone is expressly forbidden.

The publisher does not give any warranty express or implied or make any representation that the contents will be complete or accurate or up to date. The accuracy of any instructions, formulae and drug doses should be independently verified with primary sources. The publisher shall not be liable for any loss, actions, claims, proceedings, demand or costs or damages whatsoever or howsoever caused arising directly or indirectly in connection with or arising out of the use of this material.

## Estimation of the kinetic energy dissipation in fall-arrest system and manikin during fall impact

John Z. Wu\*, John R. Powers, James R. Harris and Christopher S. Pan

*National Institute for Occupational Safety and Health, Morgantown, WV 26505, USA*

*(Received 23 April 2010; final version received 15 December 2010)*

Fall-arrest systems (FASs) have been widely applied to provide a safe stop during fall incidents for occupational activities. The mechanical interaction and kinetic energy exchange between the human body and the fall-arrest system during fall impact is one of the most important factors in FAS ergonomic design. In the current study, we developed a systematic approach to evaluate the energy dissipated in the energy absorbing lanyard (EAL) and in the harness/manikin during fall impact. The kinematics of the manikin and EAL during the impact were derived using the arrest-force time histories that were measured experimentally. We applied the proposed method to analyse the experimental data of drop tests at heights of 1.83 and 3.35 m. Our preliminary results indicate that approximately 84–92% of the kinetic energy is dissipated in the EAL system and the remainder is dissipated in the harness/manikin during fall impact. The proposed approach would be useful for the ergonomic design and performance evaluation of an FAS.

**Statement of Relevance:** Mechanical interaction, especially kinetic energy exchange, between the human body and the fall-arrest system during fall impact is one of the most important factors in the ergonomic design of a fall-arrest system. In the current study, we propose an approach to quantify the kinetic energy dissipated in the energy absorbing lanyard and in the harness/body system during fall impact.

**Keywords:** fall-arrest equipment; energy; impact; drop test; lanyard

### 1. Introduction

For many years, fall-arrest systems (FASs) have been deployed to provide a safe stop during fall incidents. Different federal regulatory agencies or consensus standard organisations recommend or mandate the use of an FAS in certain cases. For example, Occupational Safety and Health Administration (OSHA) regulations (1926.451 (g) (1) (vii)) mandate the use of personal fall-arrest systems or guardrail systems as primary safety controls for scissor lifts (OSHA, 1998), which are designated as mobile scaffolds under OSHA regulations (OSHA, 1999). It is widely acknowledged that the dynamic performance of an FAS is important for personal safety. However, despite numerous fall tests and measurements of the FAS by different manufacturers and researchers over the past 60 years, much is still unknown regarding kinetic energy dissipation during fall-arrest impact.

Since it is generally accepted that it is the maximum impact force and maximum acceleration that cause death and injuries in falls (e.g. De Haven, 1942; Glaister, 1978; King, 1993), previous studies of FASs concentrated mostly on impact force and acceleration. From the early studies conducted by the Boeing company in the 1960s (Boeing, 1967), the early analysis by Wang (1977), and more extensive studies by

Sulowski and Brinkley (1990), to the most recent studies by Baszczyński (2004), all previous investigators analysed mainly the time histories of the accelerations and forces and their dependence on other factors, such as weather conditions (Baszczyński, 2004) and test surrogates (Riches, 2002). The testing instrumentation and requirements of FASs have been specified in the current US consensus standard – ANSI/ASSE Z359.13 (American National Standards Institute & American Society of Safety Engineers, 2009) – to quantify these parameters in experiments. Specifically, sampling frequencies of at least 1000 Hz are required with a response band corner frequency of 100 Hz; the load cell for measuring maximum arrest force must be able to capture peak loads of at least 15 kN; and the minimum natural frequency for the drop test structure should be 200 Hz. All these previous studies and standards contributed to refining the techniques so that current drop tests can reliably measure impact forces and accelerations during impact falls.

An FAS typically consists of three parts (Riches, 2002): a full-body safety harness, a lifeline, and connectors. The safety harness is worn by the worker and is used to distribute the dynamic loading to the human body and to maintain the human body in an

\*Corresponding author. Email: [jwu@cdc.gov](mailto:jwu@cdc.gov)

erect position with the head pointing upwards after a fall. The dynamic forces will be distributed to the sub-pelvic region of the body during a fall impact by wearing the full-body harness. The vital element of an FAS is the lifeline, which typically contains a lanyard and an energy absorber – frequently called an *energy absorbing lanyard* (EAL). The EAL absorbs the kinetic energy of the impact fall and also helps limit falling distances. During the deceleration phase of the fall, the EAL deploys and impact energy is dissipated in the EAL. The EAL helps reduce the kinetic energy absorbed by the human body, thereby reducing the impact force. The kinetic energy absorbed in the EAL is one of the important parameters for the dynamic performance of an FAS.

It is generally recognised that the interaction between the human body and a full-body harness is one of the most important factors that affect the performance of the fall-arrest system (Hsiao *et al.* 2003). The fitting of the harness to the body may influence the distribution of the impact force on the human body, thereby affecting impact kinetic energy exchange between the fall-arrest system and the human body. Sizing and fitting of the fall protection harness have been extensively investigated in previous studies (Hsiao *et al.* 2007, 2009b,a). However, how the sizing and fitting of a fall-arrest harness would influence the FAS's performance has not yet been evaluated quantitatively.

In a few studies (e.g. Gravitec, 2007), the kinetic energy dissipated in the EAL has been quantified. The energy absorbed in the EAL was usually estimated by using the product of the average arrest force and the deployment stretching of the EAL in previous studies. Physically, such a calculation is precise only when the deployment force does not vary with the deployment distance during the impact. The dynamics of the FAS and the human body during fall impact have not been systematically analysed theoretically. The purpose of the current study is to analyse the mechanical interaction and the kinetic energy exchange between the human body and the fall-arrest system during fall impact. Specifically, we are going to develop a systematic approach to evaluate the kinetic energy dissipated in the EAL and in the manikin during fall impact.

## 2. Methods

### *Dynamics of a drop test*

In any moment  $t$  during the drop of a test surrogate (Figure 1A), the dynamic balance of the test surrogate is formulated as follows:

$$T(t) + F_e(t) - mg = ma(t), \quad (1)$$

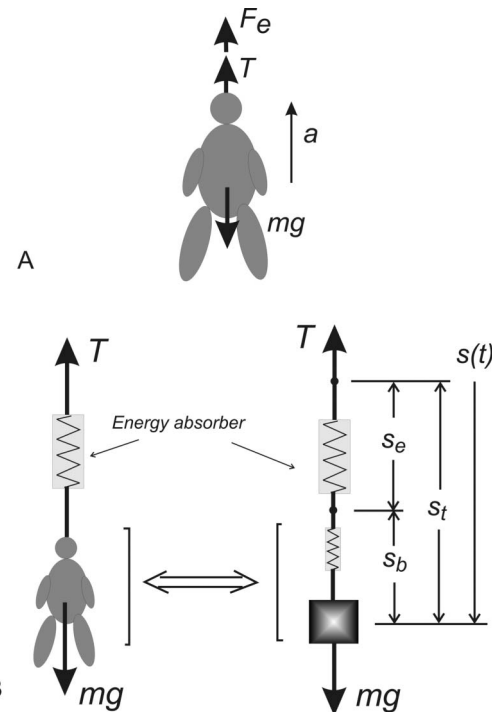


Figure 1. Modelling of the fall-arrest system (FAS). (A) Dynamic force balance in a typical fall-arrest test. (B) Modelling of the energy absorber lanyard (EAL) for the drop test. The falling manikin has a mass  $m$  and acceleration  $a$ . The fall is arrested by force  $T$  and the manikin is supported by the electro-magnetic force  $F_e$  before the drop. The EAL is mechanically equivalent to a nonlinear spring/damper element, whereas the manikin is mechanically equivalent to a system composed of a dead mass and a nonlinear spring/damper element. The total stretching of the fall system  $S_t$  consists of the stretching of the lanyard  $S_e$  and the stretching/displacement of the harness/manikin  $S_b$ .

where  $m$  and  $a$  are the mass and acceleration of the test surrogate, respectively;  $g$  ( $=9.81 \text{ m s}^{-2}$ ) is the gravitational acceleration due to the Earth;  $T$  is the arrest force in the lifeline, and  $F_e$  is the support force that holds the fall surrogate before the drop. The effects of air friction are neglected in the analysis.

Assuming that the measurements are begun at  $t = 0$ , that the supporting system is released at  $t = t_0$ , and that the test surrogate begins to fall immediately after the release of the supporting system,  $F_e$  can be precisely defined in an experiment. For  $0 < t \leq t_0$ ,  $a = 0$  and  $F_e = mg$ ; and for  $t > t_0$ ,  $F_e = 0$ . Therefore, there are only two variables,  $T$  and  $a$ , which govern the dynamics of the test surrogate during the drop and impact. In fact, we need only one of these two variables to describe the dynamics of the test surrogate, because  $T$  and  $a$  are co-related via Equation (1). If the body acceleration  $a$  is measured in a test, the arrest force  $T$  can be determined by

$$T(t) = m[a(t) + g] - F_e(t). \quad (2)$$

If the arrest force  $T$  in the lanyard is measured, the body acceleration  $a$  can be determined as well:

$$a(t) = \frac{T(t) + F_e(t) - mg}{m}. \quad (3)$$

The tension in the lanyard,  $T$ , is equal to zero when it is relaxed. Assuming that the tension in the lanyard develops for  $t \geq t_i$  ( $T = 0$  for  $t \leq t_i$  and  $T \geq 0$  for  $t > t_i$ ), Equation (3) is rewritten as

$$a(t) = \frac{T(t) - mg}{m}, \quad \text{for } t > t_i. \quad (4)$$

It is to be noted that, during a drop test,  $a(t)$  starts to increase from  $-g$  at  $t = t_i$  and  $T = 0$ , it crosses zero at  $t_a$  when  $T = mg$ , becomes positive with  $T > mg$ , and tends to become zero again at  $t \rightarrow \infty$  with  $T \rightarrow mg$ .

We are only interested in the dynamics of the test surrogate for  $t > t_i$  in the analysis, since the kinematics of the surrogate for  $t \leq t_i$  is well defined:

$$a = \begin{cases} 0, & t \leq t_0 \\ -g, & t_0 < t \leq t_i. \end{cases} \quad (5)$$

For  $t > t_i$ , the kinematics of the falling subject are determined from Equation (4):

$$v(t) = \int_{t_i}^t \frac{T(\tau) - mg}{m} d\tau - g(t_i - t_0) = \bar{v}(t) + v_i \quad (6)$$

$$s(t) = \int_{t_i}^t \bar{v}(\tau) d\tau - \frac{1}{2}g(t_i - t_0)^2 = \bar{s}(t) + s_i, \quad (7)$$

where  $v(t)$  and  $s(t)$  are the speed and displacement of the falling body, respectively;  $v_i = -g(t_i - t_0)$  and  $s_i = -\frac{1}{2}g(t_i - t_0)^2$  are the initial speed and displacement, respectively, before the tension in the lanyard develops; and

$$\bar{v}(t) = \int_{t_i}^t \frac{T(\tau) - mg}{m} d\tau \quad \text{and} \quad \bar{s}(t) = \int_{t_i}^t \bar{v}(\tau) d\tau.$$

Assuming that  $s(t)$  reaches its maximum,  $s_m$ , at  $t = t_m$ , the kinetic energy dissipated in the falling system during the impact,  $E_t$ , can be theoretically calculated by  $E_t = \int_{s_i}^{s_m} T(s) ds$  with  $s_i = s(t_i)$  and  $s_m = s(t_m)$  being the displacement at the start of EAL stretching and at the maximum of  $s(t)$ , respectively. In

practical applications, the start of the lanyard stretch is difficult to determine precisely, because there is substantial noise when the tension in the lanyard starts to develop from zero. Therefore, the stretch period is defined from  $t_a$  to  $t_m$ ; i.e. the period during which the tension in the lanyard increases from  $T(t_a) = mg$ :

$$E_t = \int_{s_a}^{s_m} T(s) ds, \quad (8)$$

where  $s_a = s(t_a)$ ; and  $t_a$  is the time when the acceleration reaches zero or when  $T = mg$ .

The relationship between the tension and displacement,  $T(s)$ , can be obtained by eliminating time,  $t$ , using  $s(t)$  obtained from Equation (7) and  $T(t)$  measured in the experiment. The maximal displacement,  $s_m = s(t_m)$ , can be determined by finding  $t_m$  from  $v(t_m) = 0$ .

From a mechanical point of view, the entire falling system consists of the energy absorber (EAL) and the falling body, as illustrated in Figure 1B. The entire kinetic energy during the impact is dissipated partially in the EAL and partially in the falling body, i.e. in the safety harness system and in the soft tissues of the human body. It is technically difficult to determine precisely the time history of the stretch of the EAL during the impact. If the maximal stretch of an EAL is known, the time histories of EAL stretching during the impact can be estimated by assuming it to be proportional to the stretch displacement of the mass centre ( $s_t(t)$ ):

$$s_e(t) = L_{\text{EAL}} \frac{s(t) - s_a}{s_m - s_a} \quad (9)$$

$$s_b(t) + s_e(t) = s_t(t) = s(t) - s_a,$$

where  $L_{\text{EAL}}$  is the maximum stretch of the EAL;  $s_a = s(t_a)$  and  $s_m = s(t_m)$  are the displacements of the mass centre at  $t = t_a$  and  $t = t_m$ , respectively;  $s_e(t)$ ,  $s_b(t)$  and  $s_t(t)$  are the time histories of the stretch displacement of the EAL, the stretch displacement of the harness/manikin body, and the total stretch displacement at the mass centre during the impact, respectively, as illustrated in Figure 1B. It is to be noted that the stretch of the EAL,  $s_e(t)$ , increases from 0 to  $L_{\text{EAL}}$  during the time period from  $t_a$  to  $t_m$ .

Consequently, the total impact kinetic energy  $E_t$  and the kinetic energy dissipation in the EAL,  $E_e$ , and in the falling body,  $E_b$ , can be calculated by

$$E_t = \int_{s_a}^{s_m} T(s) ds = E_e + E_b, \quad (10)$$

where

$$E_e = \int_{s_e(t_a)}^{s_e(t_m)} T(s_e) ds_e, \quad E_b = \int_{s_b(t_a)}^{s_b(t_m)} T(s_b) ds_b. \quad (11)$$

For a given  $t$ ,  $s_e(t)$  and  $s_b(t)$  are determined via Equation (9) and  $T(t)$  is known from the experimental data. The relationships,  $T(s_e)$  and  $T(s_b)$ , can be found numerically and plotted graphically.

If the air friction is neglected, the power absorption in EAL ( $P_e$ ), in the falling body ( $P_b$ ), and in the entire falling system ( $P_t$ ) can be estimated by

$$P_e = T \frac{ds_e(t)}{dt}, \quad P_b = T \frac{ds_b(t)}{dt} \quad \text{and} \\ P_t = T \frac{ds(t)}{dt} = P_e + P_b. \quad (12)$$

## 2. Experimental set-up and procedure

The experimental set-up is illustrated in Figure 2. An advanced dynamic anthropomorphic manikin (Large ADAM™, Veridian, Dayton, Ohio, USA) was used as the test surrogate in the study. The manikin has a mass of 108 kg and a height of 1.88 m. The manikin accelerations were measured via built-in uni-axial accelerometers (Entran EAX series) at three locations,

i.e. at the head, middle of the spine, and torso. The test manikin was dropped from a scissor lift (Model SJIII3219, SkyJack, Guelph, ON, Canada). The scissor lift was lifted to its full height extension of 5.79 m and the base was secured to prevent tip-over. The drop test data used in the current analysis were obtained in our previous study to evaluate the FAS influence on the stability of the scissor lift (Harris *et al.* 2010).

Before the drop test, the manikin was held by an electro-magnetic drop control mechanism that was attached to a 49 kN crane. The crane could move the manikin to control the dropping height, as well as to adjust the drop location.

Standard energy absorbing lanyards (EALs) (Workman™, Model 10072474, MSA, Pittsburgh, PA, USA) and matching safety harnesses (Workman™, Model 10072479, MSA, Pittsburgh, PA, USA) were used in the study. A load cell (13.4 kN, S-type, Interface Inc., Scottsdale, Arizona, USA) was placed in line with the energy absorbing lanyard to measure the arrest force, as shown in Figure 2B. The lanyard was connected at the midspan of the top-rail. The load cell was connected to the lanyard via a sling hook, which may slightly contact with the guardrail during the test. The hookup location of the load cell and the lanyard was carefully kept aligned during the test, so that the effect of sling hook-guardrail contact on the force measurement was negligible.

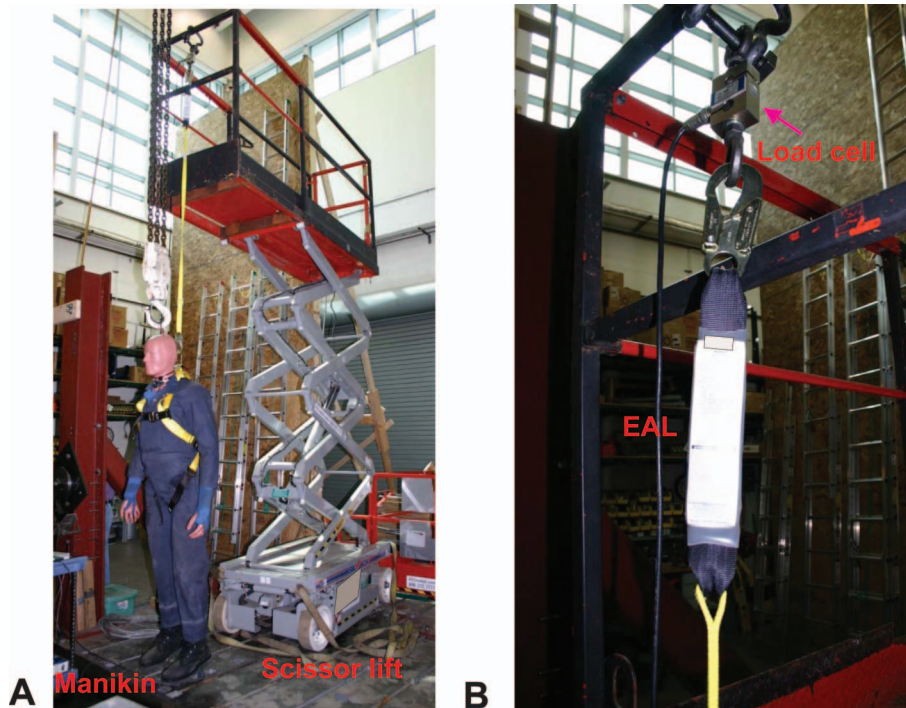


Figure 2. The experimental set-up for the fall-arrest test. An advanced dynamic anthropomorphic manikin (Large ADAM™, Veridian, Dayton, Ohio, USA) was dropped from a scissor lift (Model SJIII3219, SkyJack, Guelph, ON, Canada). (A) The scissor lift and the manikin. (B) Attachment of the load cell and energy absorbing lanyard (EAL) to the scissor lift.

The length of the EAL was measured manually by using a steel tape before and after the drop tests. The length difference was considered as the stretch of the EAL,  $L_{EAL}$ . In the length measurements, each of the EALs was hung on a stable structure with an attached rigid weight that was equivalent to the body weight of the manikin.

The test system was controlled by a computer via a LabView (version 7.1, National Instruments, Inc., Austin, Texas, USA) program. The program was used to trigger the data acquisition as well as to control the release of the electro-magnetic drop mechanism. The drop test was initiated remotely via the control computer by a test engineer. The force data was sampled at 1000 Hz, whereas the ADAM accelerations were sampled at 10,000 Hz. The manikin was

dropped from two different heights with nominal drop heights of 1.83 and 3.35 m. The nominal drop height of 3.35 m represents the drop distance that an operator standing on the midrail of the scissor lift would fall.

### 3. Results

The time histories of the support force, body accelerations, and arrest force for the  $h_1$  and  $h_2$  drop tests are shown in the left and right columns of Figure 3, respectively. In order to illustrate the data processing procedure, we set  $t = 0$  at the start of data recording. In these figures, the time histories of the support force  $F_c(t)$  are prescribed and the time histories of the body acceleration  $a(t)$  are measured

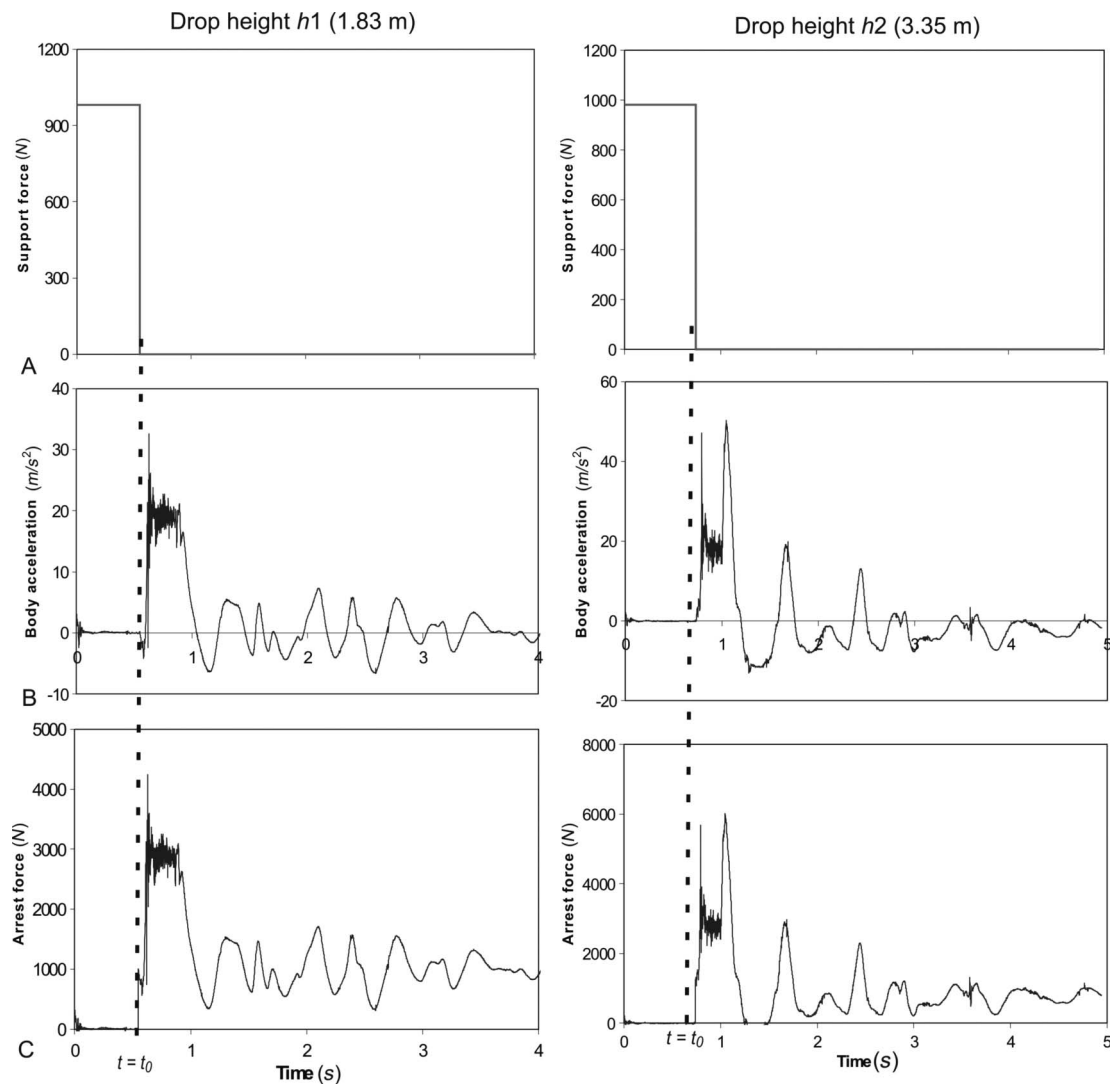


Figure 3. Representative time histories of support force  $F_c$ , body acceleration  $a$ , and arrest force  $T$  for the drop test. The support force was prescribed and the acceleration was measured, whereas the arrest force was calculated.

experimentally, whereas the time histories of the arrest force  $T(t)$  are calculated via Equation (2). The figures show that the fall of the manikin starts at  $t = t_0$ , when  $F_c(t)$  becomes zero.

The arrest-force values calculated using the kinematic data are compared with those measured directly via the load cell for the  $h1$  and  $h2$  drop tests, as shown in Figure 4. Our results show that the peak values of the calculated arrest forces differ from those of the measured arrest forces by less than 5%.

Using the time histories of the arrest forces, which were measured via the load cell, the time histories of the acceleration, speed and displacement of the falling manikin were calculated using Equations (4) and (6)–(7). The arrest force, body acceleration, speed and displacement for the  $h1$  and  $h2$  drop tests are shown in Figure 5 in the left and right columns, respectively. The time when the tension in EAL starts to increase ( $t_i$ ), the time when the body acceleration becomes zero the first time ( $t_a$ ), and the time when the falling manikin reaches its extreme position ( $t_m$ ) were identified from these analyses.

The body accelerations calculated using the force data differ from those measured directly via the accelerometers mounted on the manikin by less than 10% at peak and by less than 5% at EAL deployment, as illustrated in Figure 6. These results suggest that the dynamics of the falling body could be predicted

using the arrest-force data within an acceptable error range.

The period of the EAL deployment is defined as the time period between  $t_a$  and  $t_m$ , as marked on the time histories of the arrest force for the  $h1$  and  $h2$  drop tests in Figure 7A. Both the results of the  $h1$  and  $h2$  drop tests showed that the stretch periods end when the arrest forces just pass their maximum points.

The travel distance of the falling body and the stretch of the EAL during the impact are evaluated and shown in Figure 7B. The total displacements of the falling manikin were taken from the results shown in Figure 5, and the stretch time histories of the EAL during the impact were estimated using Equation (9). The values of the maximum stretch of the energy absorber,  $L_{EAL}$ , were measured.

The relationships of the arrest force as a function of the body displacement, the EAL stretching, and the mass centre displacement for both tests were evaluated and plotted in Figure 7C. This figure shows that the arrest forces initially increase with increasing stretch and then stay almost unchanged during EAL deployment. The arrest force jumps suddenly by the end of the stretch period for the  $h2$  drop test, while it shows no such force jump for the  $h1$  drop test.

The time histories of the power absorption in the EAL ( $P_e$ ) and in the manikin ( $P_b$ ) for the  $h1$  and  $h2$  drop tests are calculated using Equation (12) and are shown in Figure 8. The power absorptions during the impact increase rapidly when the deployment of the EAL starts, reaches the first peak around the time when the deployment force reaches the designed deployment force ( $F_{ave}$ ) and then decreases to around zero towards the end of the impact. For the  $h2$  drop test (Figure 8B), there is a second peak in the power absorption, which corresponds to the peak force around the time when the EAL is fully deployed. The results show that the peak energy absorption in the EAL is approximately 11 and 5 times that in the manikin body for the  $h1$  and  $h2$  drop tests, respectively.

The effective drop height  $h_{eff}$  was the actual drop height in the drop tests. Due to the restriction of the test set-up,  $h_{eff}$  is a little greater than the nominal drop height ( $h$ ) for the  $h2$  drop test. The maximal stretch displacement of the body mass centre ( $S_b = s_b(t_m)$ ) and the maximal stretch of the EAL ( $L_{EAL}$ ), together with the effective drop height ( $h_{eff}$ ), are listed in Table 1. Using these data, the potential drop energy for the tests was calculated by  $E_p = mg(h_{eff} + S_b + L_{EAL})$  and listed in the table.

Finally, the kinetic energies dissipated in the entire system ( $E_i$ ), in the EAL ( $E_e$ ), and in the manikin body ( $E_b$ ), for both tests were evaluated via Equations (8)–(11) and listed in Table 1. The kinetic energies,

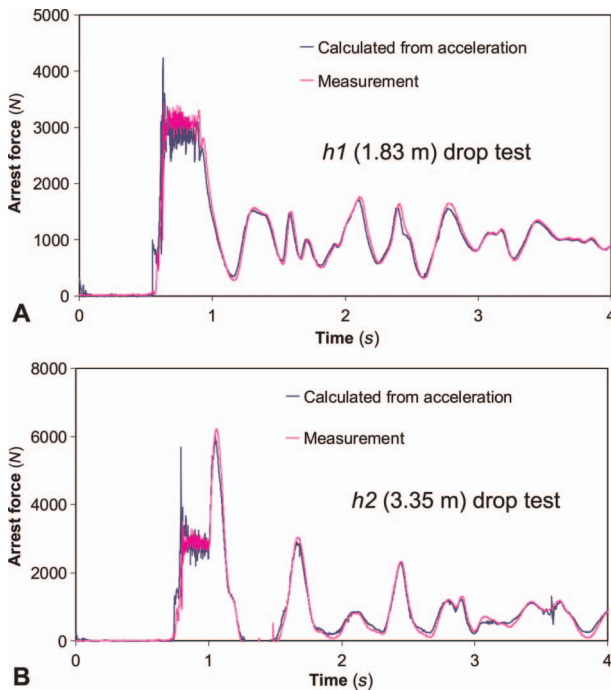


Figure 4. The time histories of the calculated arrest force compared with those of the experimentally measured force. (A)  $h1$  (1.83 m) drop test. (B)  $h2$  (3.35 m) drop test.

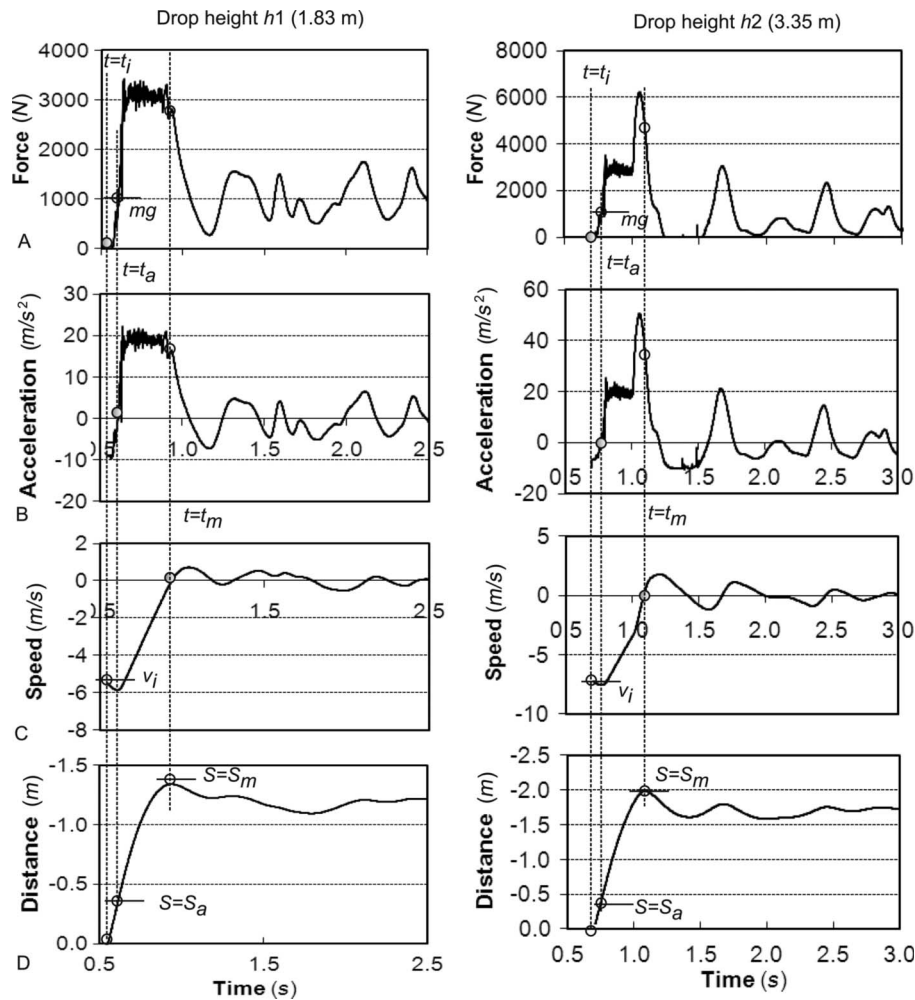


Figure 5. The time histories of the arrest force  $T$ , body acceleration  $a$ , speed  $v$  and travel distance  $s$ . The arrest force was measured, whereas the acceleration, speed and travel distance of the falling body were calculated;  $t_i$ ,  $t_a$  and  $t_m$  represent the time that the arrest force starts to increase, the time that the lanyard stretch starts, and the time that the lanyard stretch reaches its maximum, respectively.  $v_i$  is the speed at  $t_i$ , and  $S_a$  is the travel distance at  $t_a$ .  $S_m$  is the maximal travel distance during fall impact, which is the travel distance at  $t_m$ .

$E_t$  and  $E_e$ , were integrated from the curves of  $T(s_i)$  and  $T(s_e)$  (Figure 7C), as described in Equations (8)–(11). It is seen that the total impact energy increased by 42% (from 2903 to 4116 J), while the percentage of the kinetic energy dissipated in the EAL decreased from 92 to 84%, which resulted in a 193% increase of the kinetic energy dissipation in the manikin body (from 230 to 674 J), as the drop height increased from 1.83 to 3.35 m in the tests.

The current results show that the percentage of the potential drop energy consumed in the manikin–harness–EAL system during fall impact decreased from approximately 97 to 81% when the drop height increased from 1.83 to 3.35 m (Table 1).

In order to verify the proposed approach, we have performed a drop test at a height of 3.35 m using a rigid weight (mass 128.6 kg), as described in Appendix

A in detail. The test set-up of the rigid-weight drop is the same as the manikin drop tests, except that the EAL is attached directly onto the rigid weight. Our results (Figures A1 and A2) show that the time history of the stretch displacement of the mass centre of the rigid weight calculated using the proposed approach is consistent with that of the lanyard stretch, which was measured experimentally. The kinetic energy absorbed in the system (5737.3 J) is identical with that in the EAL (5664.5 J) as well, as shown in Table A1.

#### 4. Discussion and conclusion

The kinetic energy dissipation during fall impact is an important parameter that characterises the dynamic performance of an FAS. In the previous studies, the

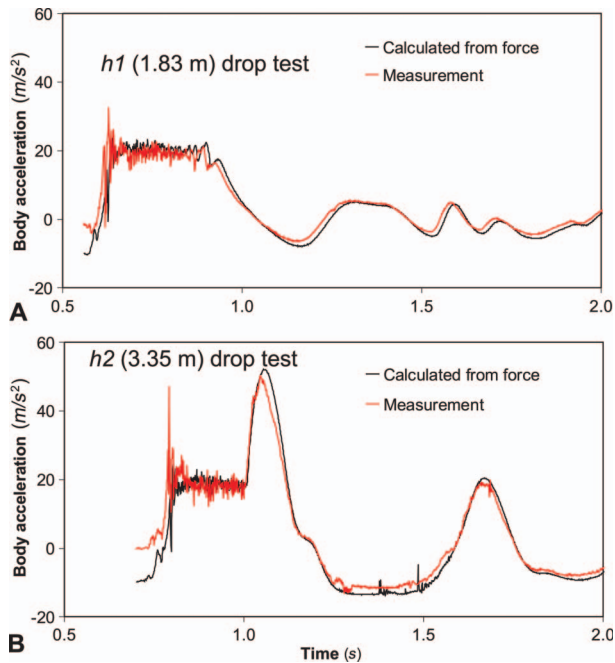


Figure 6. The time histories of the calculated acceleration  $a$  compared with those measured directly via accelerometers. (A)  $h_1$  (1.83 m) drop test. (B)  $h_2$  (3.35 m) drop test.

dynamics and impact kinetic energy during fall impact have not been systematically analysed. In the current study, we propose an approach to quantify systematically the kinetic energy dissipated in the EAL and in the falling body during fall impact. We analytically derived the relationships between the deployment force, the lanyard stretch, and the manikin body motion during fall impact. The proposed method needs only the arrest-force time history data to derive the kinetic energy dissipations. Since the arrest force in the EAL is measured routinely in dynamic performance tests in fall-arrest system industries, the proposed approach can be applied by engineers to evaluate the dynamic performance of FASs, thereby providing valuable information for research into and development of related safety products.

Our results show that arrest forces calculated using the kinematic data agree well with those measured directly via the force sensor (Figure 4) and the accelerations calculated using the force data agree well with those measured directly (Figure 6). These analyses indicate that the kinematics of the manikin can be determined using measured arrest forces, and the arrest force in the EAL can also be determined using accelerations measured at the manikin. Although our observations show that the kinetics of the system during fall impact can be fully described using either arrest force measurements in the EAL or acceleration of the surrogate, the kinematics calculated using the

force data may more precisely reflect the dynamic characteristics of the manikin motions than those calculated using acceleration data. This is because the measured accelerations may not reflect the motions of the ‘true’ mass centre of the falling body due to flexibility and postural changes of the manikin during impact. Theoretically, the kinematics derived from the force will strictly reflect the motion of the ‘true’ mass centre, even when the body is deformable and the relative position of the mass centre varies in motion.

Our preliminary results (Table 1) indicate that roughly 84–92% of the impact kinetic energy is dissipated in the EAL and the remainder is dissipated in the falling body, including the harness system and manikin body. The effects of the impact intensity on the kinetic energy distributions between the EAL and the human body has yet to be studied via further tests and analysis.

Our results indicate that the deployment of the EAL during fall-arrest impact can be typically characterised in three stages (Figure 7A). In the initial impact stage, the arrest force increases with increasing deployment distance of the EAL. The second stage is a stationary stage, in which the arrest force stays nearly constant around the average deployment force ( $F_{ave}$ ) while the EAL deployment displacement increases. The arrest force then increases dramatically with increasing deployment displacement in the third impact stage. For the fall-arrest test with a small impact force, such as in the case of the  $h_1$  drop test (Figure 7), the EAL will not be fully deployed during impact and the third stage does not appear. The average deployment force ( $F_{ave}$ ) is probably associated with the structural characteristics of the EAL system and does not depend on the impact tests. This is manifested in our results, which show that the relationships between force and EAL-stretch (Figure 7C) and the time history of power absorption in the EAL (Figure 8) exhibit the same patterns before the EAL is fully deployed for both the  $h_1$  and  $h_2$  drop tests. Despite a 69% difference in potential drop energy (Table 1) in these two tests, the deployment forces ( $F_{ave}$ ) (Figure 7A) differ by less than 6% (Table 1). These results suggest that the characteristics of EALs can probably be described using the force-stretch relationship.

Using the average method due to Gravitec (2007), the kinetic energy dissipated in the EAL during impact is estimated by  $E = F_{ave}L_{EAL}$ . The impact energies in the EAL calculated using these two different methods differ by less than 6 and 1% for the  $h_1$  and  $h_2$  drop tests, respectively (Table 1). Our results confirm that the average method gives a good estimation for the impact energy dissipations in the EAL. However, the

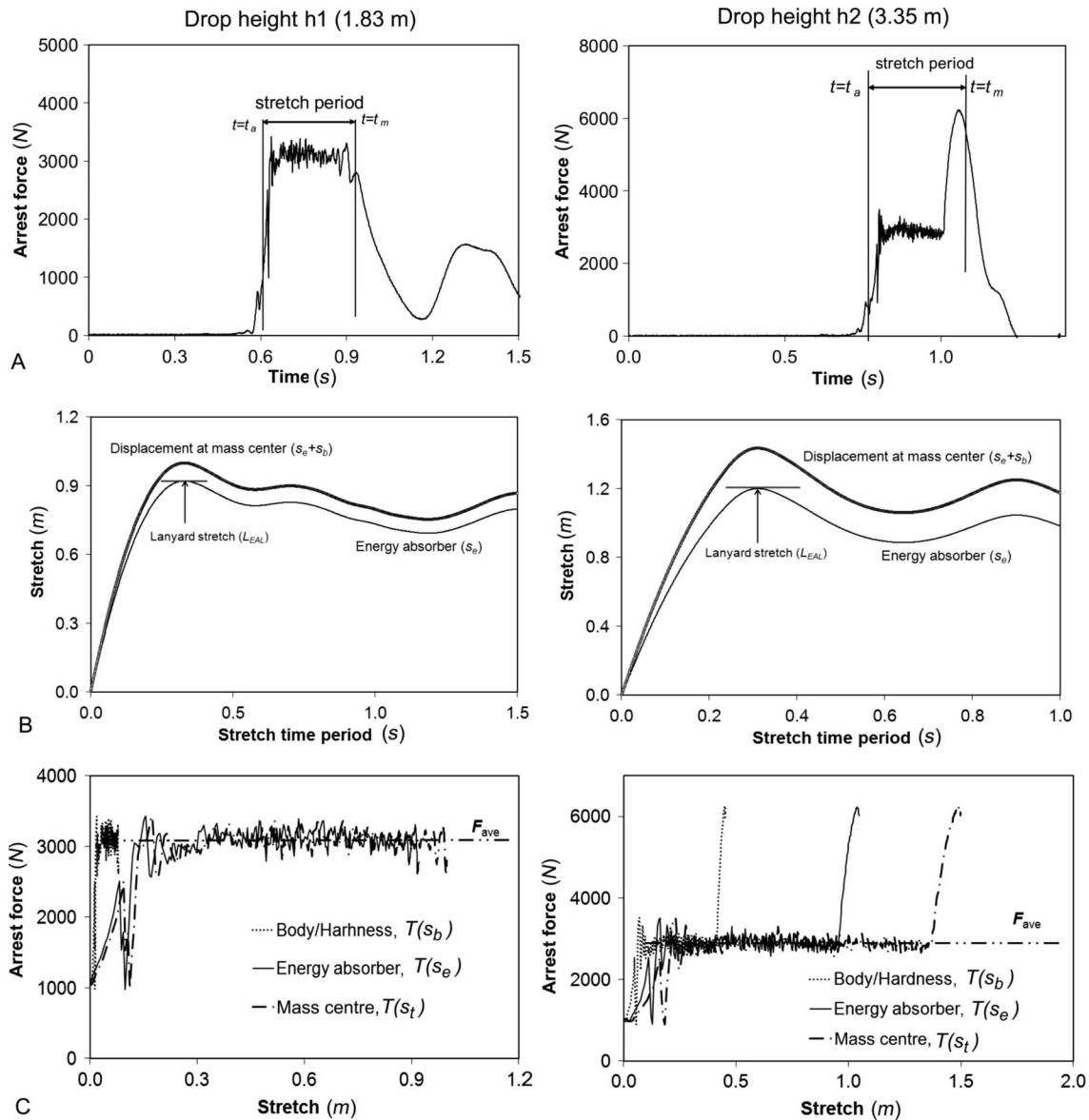


Figure 7. The stretching of the energy absorber lanyard (EAL). (A) The definition of the stretch period in the time histories of the arrest force. (B) The time histories of lanyard stretching and the travel distance of the mass centre during fall impact. (C) The arrest force  $T$  as a function of the body/harness deformation, lanyard stretch, and total mass centre displacement.

average method cannot be applied to estimate the impact energy dissipated in the manikin or human body.

Using the proposed approach, the EAL deployment period is defined as the time period between  $t_a$  and  $t_m$ . The parameter  $t_a$  is the time when the tension in the EAL reaches the static body weight and is defined as the time when the acceleration becomes zero. The parameter  $t_m$  is the time when the stretch of the system (including the EAL, safety harness and falling surrogate) reach the maximum, and is defined by the moment when the speed becomes zero. It is interesting to see that  $t_m$  is not the time when the arrest

force reaches its maximum, but the time when the arrest force just passes its maximum value (Figure 5).

Theoretically, EAL stretching starts from  $t_i$ . The length of EAL at  $t_i$  – the natural length – is difficult to measure consistently in practice, because the EAL does not stay straight at zero loading. Consequently, there is substantial noise when the tension in the lanyard starts to develop from zero. If the stretch period of the EAL is defined as the time period ( $t_m - t_a$ ), as in this study, the EAL stretching can be measured consistently in tests. It should be noted that the majority of the displacement occurring during the period ( $t_a - t_i$ ) was due to the loose harness of the manikin body and the

relaxation of the EAL, not the elastic deformation of the EAL. It should be noted that some of the elastic energy in the EAL is ignored by defining the stretch period as  $(t_m - t_a)$ .

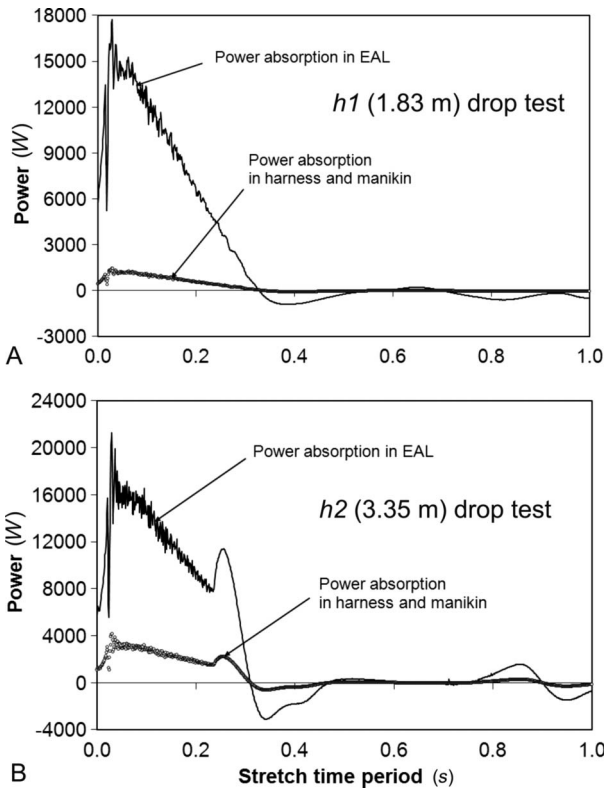


Figure 8. The time histories of the power absorption in the lanyard and manikin body. (A)  $h_1$  (1.83 m) drop test. (B)  $h_2$  (3.35 m) drop test.

One of the error sources in acceleration measurement may come from the mis-alignment of the built-in uni-axial accelerometer and displacement. Our results showed that the directly measured accelerations differ from those calculated from the force by less than 5% at peaks (Figure 6), indicating that the error in the directly measured acceleration due to mis-alignment is within an acceptable range.

One simplifying assumption we made in calculating the time histories of EAL stretching is that EAL stretching is considered to be proportional to the displacement of the mass centre (Equation 9). It is to be noted that at the boundary points,  $t = t_a$  and  $t_m$ , the EAL stretching is known and is equal to 0 and  $L_{EAL}$ , respectively. The error introduced by the proportionality assumption is only the shape of the curve  $T(s)$  for the time period  $t_a < t < t_m$ , or  $s(t_a) < s(t) < s(t_m)$ . It would certainly be possible to make a more complex model by assuming that EAL stretching is nonlinearly proportional to the displacement of the mass centre. However, if the majority of the mass centre displacement is due to EAL stretching (approximately 87–92% of the total mass centre displacement is contributed by EAL stretching in the current analysis), the error because of this simplifying assumption should be limited and negligible when compared with other experimental uncertainty.

In the current analysis, EAL stretching under dynamic loading was approximated by using the EAL stretching measured under static loading ( $L_{EAL}$ ). The EAL stretching under dynamic loading should be greater than that measured statically due to dynamic elastic deformation. The rigid-weight drop test described in Appendix A was used to quantify the

Table 1. Summary of the experimental data and analysis results. The total impact energy ( $E_t$ ) is calculated via Equation (10). The impact energy absorbed in EAL ( $E_e$ ) is calculated via Equation (11). The effective drop height ( $h_{eff}$ ) for the  $h_2$  (3.35 m) drop test was 0.022 m greater than the nominal drop height ( $h = h_2$ ).

Parameters	Units	Test	
		$h_1$ drop	$h_2$ drop
Nominal drop height, $h$	m	1.83	3.35
Effective drop height, $h_{eff}$	m	1.83	3.49
Maximal stretch displacement of harness/manikin, $S_b$	m	0.08	0.23
Lanyard deployment stretch, $L_{EAL}$	m	0.92	1.20
Average deployment force, $F_{ave}$	N	3067.0	2883.6
Maximal arrest force, $F_{max}$	N	3431.7	6227.1
Potential drop energy, $E_p = mg(h_{eff} + S_b + L_{EAL})$	J	2999.0	5070.6
Impact energy absorbed in lanyard, $E_e$	J	2672.7	3441.4
Impact energy absorbed in harness/manikin body, $E_b$	J	230.1	674.1
Total impact energy absorbed in falling system, $E_t = E_e + E_b$	J	2902.8	4115.5
Portion of impact energy absorbed in lanyard, $E_e/E_t$	%	92.1	83.6
Portion of impact energy absorbed in harness/manikin body, $E_b/E_t$	%	7.9	16.4
Portion of potential drop energy consumed in impact, $E_t/E_p$	%	96.8	81.2
Portion of potential drop energy dissipated in structure $(E_p - E_t)/E_p$	%	3.2	18.8

difference between  $L_{EAL}$  and EAL dynamic stretching. In the rigid-weight drop test, the EAL was directly attached to the rigid weight – no effects of the harness attachment and body deformation were involved. Our results suggest that the dynamic maximal stretching can be well estimated by using  $L_{EAL}$  (with an error of less than 1%, as shown in Figure A2).

The load cell was connected to the lanyard via a sling hook in the current experimental set-up. The sling hook may slightly contact the guardrail during the test. We carefully adjusted the hookup location such that the load cell and the lanyard were kept aligned during the test. In addition, the friction between the sling hook and the guardrail – both are made of steel – is very small. Therefore, any error in the force measurement due to sling hook–guardrail contact is negligible.

It should be noted that the manikin was dropped from a scissor lift in the current study. The natural frequency of the scissor lift is far less than 200 Hz, which is required for the drop test structure as specified in ANSI/ASSE Z359.13 for the standardised drop test conditions. In fall-arrest tests conducted on the scissor lift, a portion of the potential drop energy will be dissipated in the structure of the scissor lift, especially for a high impact force. This is demonstrated in our test results (Table 1): the percentage of the potential drop energy converted to the kinetic energy of the falling system during the drop tests reaches approximately 97 and 81%, for the  $h1$  and  $h2$  drop tests, respectively. Since the proposed method is independent of the drop test structure, it can also be applied to estimate the energy dissipations for any standardised and non-standardised drop tests.

### Disclaimers

Mention of product and/or company names does not imply endorsement by the National Institute for Occupational Safety and Health. The findings and conclusions in this paper are those of the authors and do not necessarily represent the views of the National Institute for Occupational Safety and Health.

### Acknowledgements

We would like to acknowledge the contributions of SkyJack Inc., which provided the study with the use of a new scissor lift and other critical technical and design data. We are grateful to MSA, who generously provided the study with the use of new harnesses/lanyards. We acknowledge the International Safety Equipment Association for their constructive comments at various stages of this study. We want also to express our gratitude to Randall Wingfield and Gravitec Inc., who generously provided constructive comments concerning the drop tests. Finally, special appreciation is extended to Doug Cantis and Bradley Newbraugh (NIOSH) for their valuable assistance in data collection.

### References

- American National Standards Institute & American Society of Safety Engineers (ANSI/ASSE), 2009. Z359.13–2009. *Personal energy absorbers and energy absorbing lanyards*.
- Baszczynski, K., 2004. Influence of weather conditions on the performance of energy absorbers and guided type fall arresters on a flexible anchorage line during fall arresting. *Safety Science*, 42 (6), 519–536.
- Boeing, 1967. *Evaluation of safety-belts, lanyards and shock absorbers*. Aero-Space Division, Boeing Company, Technical Report 2-1886-09.
- De Haven, H., 1942. Mechanical analysis of survival in falls from heights of fifty to one hundred and fifty feet. *War Medicine*, 2, 586–596.
- Glaister, D.H., 1978. Human tolerance to impact acceleration. *British Journal of Accident Surgery*, 9 (3), 191–198.
- Gravitec, 2007. Material test report: 1.4 multiplier testing. *By Design*, 7 (1), 1–9.
- Harris, J.R., et al., 2010. Fall arrest characteristics of a scissor lift. *Journal of Safety Research*, 41 (3), 213–220.
- Hsiao, H., Bradtmiller, B., and Whitestone, J., 2003. Sizing and fit of fall-protection harnesses. *Ergonomics*, 46 (12), 1233–1258.
- Hsiao, H., et al., 2009a. Development of sizing structure for fall arrest harness design. *Ergonomics*, 52 (9), 1128–1143.
- Hsiao, H., et al., 2009b. Harness sizing and strap length configurations. *Human Factors*, 51 (4), 497–518.
- Hsiao, H., Whitestone, J., and Kau, T.Y., 2007. Evaluation of fall arrest harness sizing schemes. *Human Factors*, 49 (3), 447–464.
- King, A.I., 1993. Progress of research on impact biomechanics. *Journal of Biomechanical Engineering*, 115 (4B), 582–587.
- Occupational Safety and Health Administration (OSHA), 1998. *Standard interpretations – 07/21/1998 – Aerial lift regulations; fall protection for scissor lifts*.
- Occupational Safety and Health Administration (OSHA), 1999. 64:38077-38086. *Safety standards for fall protection in the construction industry*.
- Riches, D., 2002. *Analysis and evaluation of different types of test surrogate employed in the dynamic performance testing of fall-arrest equipment*. Health and Safety Executive (HSE), Contract Research Report Vol. 411/2002. Norwich, UK: HSE.
- Sulowski, A.C. and Brinkley, J.W., 1990. Measurement of maximum arrest force in performance tests of fall protection equipment. *Journal of Testing and Evaluation*, 18 (2), 123–127.
- Wang, C.H., 1977. Free-fall restraint systems. *Professional Safety* (February), 9–13.

### Appendix A

The rigid weight (mass 128.6 kg) was dropped from a height of 3.35 m. No harness was employed in the rigid-weight drop test and the EAL was attached directly on to the rigid weight. The test set-up and the data analysis procedure for the rigid-weight drop test were the same as those used for the manikin drop tests.

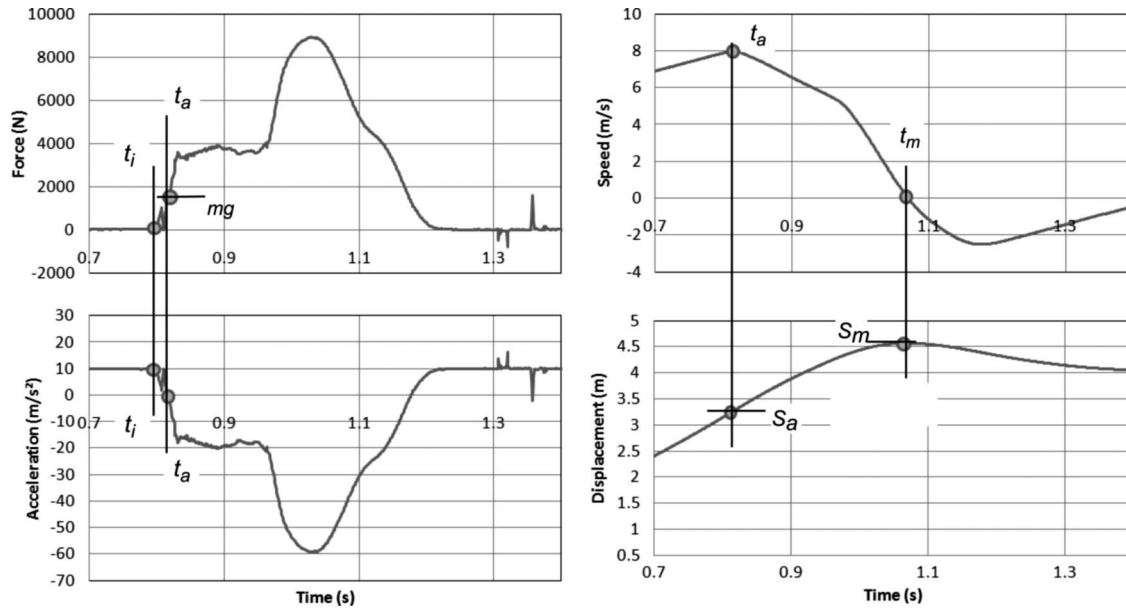


Figure A1. The time histories of the arrest force  $T$ , body acceleration  $a$ , speed  $v$ , and travel distance  $s$ , for a 3.35 m drop test using a rigid weight. The arrest force was measured, whereas the acceleration, speed, and travel distance of the falling rigid body were calculated.  $t_i$ ,  $t_a$  and  $t_m$  represent the time that the arrest force starts to increase, the time that the lanyard stretching starts, and the time that the lanyard stretching reaches its maximum, respectively.  $S_a$  is the travel distance of the mass centre at  $t_a$ , and  $S_m = s(t_m)$  is the maximal travel distance of the mass centre during fall impact.

Table A1. Summary of the analysis results for the rigid-weight drop test. The total impact energy,  $E_t$ , is calculated via Equation (10); the impact energy absorbed in EAL,  $E_e$ , is calculated via Equation (11).

Parameters	Units	
Nominal drop height, $h$	m	3.35
Effective drop height, $h_{\text{eff}}$	m	3.50
Maximal stretch displacement at mass centre, $S_t$	m	1.32
Lanyard deployment stretch, $L_{\text{EAL}}$	m	1.30
Average deployment force, $F_{\text{ave}}$	N	3627.4
Maximal arrest force, $F_{\text{max}}$	N	8924.1
Potential drop energy, $E_p = mg(h_{\text{eff}} + L_{\text{EAL}})$	J	6053.3
Impact energy absorbed in lanyard, $E_e$	J	5664.5
Total impact energy absorbed in falling system, $E_t$	J	5737.3
Portion of impact energy absorbed in lanyard, $E_e/E_t$	%	98.7
Portion of impact energy dissipated in system, $(E_t - E_e)/E_t$	%	1.3
Portion of potential drop energy consumed in impact, $E_t/E_p$	%	94.8
Portion of potential drop energy dissipated in structure, $(E_p - E_t)/E_p$	%	5.2

The arrest force, body acceleration, speed, and displacement for the rigid-weight drop test are shown in Figure A1. From the figure, the time when the tension in the EAL starts to increase ( $t_i$ ), the time when the body acceleration becomes zero for the first time ( $t_a$ ), and the time when the falling rigid weight reaches its extreme position ( $t_m$ ) were identified.

The time history of the stretch distance of the mass centre of the rigid weight is compared with that of EAL stretching in Figure A2. The stretch displacement of the rigid weight was obtained from the results shown in Figure A1, and the stretch time history of the EAL was calculated using Equation (9). Theoretically, the calculated maximal displacement of the mass

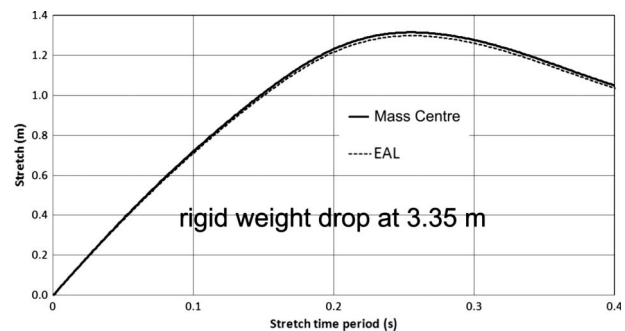


Figure A2. The time histories of the lanyard stretch and the stretch distance of the mass centre during fall impact for the rigid-weight drop test.

centre of the rigid weight,  $S_t$ , should be equal to the stretch of the EAL,  $L_{EAL}$ . The test results show that  $S_t$  differs from  $L_{EAL}$  by less than 1% (Table A1).

The kinetic energy dissipated in the falling system ( $E_t$ ) is compared with that in the EAL ( $E_e$ ) in Table A1. The kinetic impact energies,  $E_t$  and  $E_c$ , were calculated

via Equations (8)–(11). Our analysis indicates that about 99% of the impact kinetic energy is dissipated in the EAL during fall impact, confirming the proposed approach. About 95% of the potential drop energy is converted to the kinetic energy of the falling system in the rigid-weight drop test (Table A1).